PHYSICAL REVIEW B VOLUME 15, NUMBER 6 15 MARCH 1977

Optical properties of polystyrene from the near-infrared to the x-ray region and convergence of optical sum rules

T. Inagaki*
Department of Physics, Osaka Kyoiku University, Osaka, Japan

E. T. Arakawa, R. N. Hamm, and M. W. Williams
Health Physics Division, Oak Ridge National Laboratory,† Oak Ridge, Tennessee 37830
(Received 29 November 1976)

Optical properties of polystyrene in the form of thin films were determined for photon energies between 0.6 and 82 eV from transmission measurements. The results for k, the extinction coefficient, were combined with previous experimental results in the soft and hard x-ray regions up to 8050 eV. Analyses were made on several sum rules for the optical properties in this unusually wide energy range, including a sum rule for the refractive index n derived recently by Altarelli *et al.* Redistribution of the oscillator strength corresponding to 2.7% of the total electrons was found between the valence and core excitations of carbon. Using the complex dielectric function and the energy-loss function obtained, the average photoexcitation energy and the average energy loss for fast-charged particles over the entire oscillator strength distribution were evaluated to be 25.1 and 36.8 eV, respectively.

I. INTRODUCTION

The primary purpose of this paper is to examine in detail the response of electrons in a typical solid hydrocarbon to electromagnetic radiation over essentially the whole frequency range. This is achieved through sum-rule calculations which are employed to determine the way in which the oscillator strength converges. In the past such calculations and their interpretation have suffered to a greater or lesser extent because the experimental data were generally unavailable over a wide enough energy range to give the desired certainty in the required extrapolations to infinite energy. To our knowledge there are just two previous studies[1] performed on experimental data which extends over a sufficiently large energy range. We know of no such analysis for any hydrocarbon.

In this study, we report the optical properties of polystyrene $-(C_8H_8)-$, in the form of thin solid films over the range of photon energies from 0.6 to 82 eV. The results for k, the extinction coefficient, are combined with the previous experimental data from 30 to 1550 eV taken by Lukirskii *et al.*,[2] and those from 1490 to 8050 eV by Nordfors.[3] The combined spectrum of k covers substantially all the electronic excitations (more than 99.9% of the total oscillator strength), including the carbon core excitations starting at around 282 eV. Despite the recent progress in synchrotron radiation techniques, which makes it possible to obtain optical spectra from the infrared to the hard x-ray region using a continuum photon source, similar data for any kind of material are still quite rare.

In addition to the well-known f sum rules,[4] a detailed analysis is performed in this study on the refractive index n at high energies in order to employ a new sum rule for n which has been derived recently by Altarelli *et al.*[5] using the superconvergence theorem in high-energy physics. Since, as will be shown, the convergence of this sum rule is quite slow, it can be demonstrated and/or used only when the n values are available up to the extremely-high-energy region.

II. EXPERIMENTAL

Optical properties of polystyrene films between 0.6 and 82 eV were determined by the transmission method, details of which have been described previously.[6] In this method, the quantities determined experimentally are the transmittance T of a free-standing film as a function of photon energy over the whole range of photon energies, and the film thickness d. In addition the values of n are measured directly over a limited energy region where the films are transparent. To derive the optical properties n and k at each energy, the Kramers-Kronig relation between n and k is then utilized. An iterative computational procedure is carried out between the Kramers-Kronig relation and the explicit expression for transmittance which includes the correction factor for reflection effects at the film boundaries, until the values of n and k converge. n and k are thus determined self-consistently so that they reproduce the observed value of transmittance.

Self-supporting films of polystyrene were prepared by the same method as described previously.[7] Uniformity of film thickness was checked by measuring the transmittance at a suitable wavelength while scanning the whole film area. Determination of the film thickness d was made by observation of transmission maxima and minima due to interference in the transparent region. For the thinnest films, interference patterns could not be used as even the first minimum did not occur in the nonabsorbing region below 4.4 eV (above ~2800 Å). In such cases the thickness was determined directly from the explicit expression for the transmittance in the transparent ($k=0$) region[6]

$$T=\frac{[4n/(1+n)^2]^2}{1-2[(1-n)/(n+1)]^2\cos(4\pi nd/\lambda)+[(n-1)/(n+1)]^4}, \tag{1}$$

using the experimental values of T and n, where λ is the wavelength of the incident photons. The thicknesses of the five films used were found to be 380, 440, 570, 720, and 830 Å with about ±30Å uncertainty. These values were adjusted, where necessary, within the limit of the experimental uncertainty so that the final results for n in the transparent region calculated from T and d agreed with the directly measured values.

Refractive indices n between 2.0 and 4.4 eV, where polystyrene is transparent, were determined by the critical angle, Brewster angle, and interference methods using separately prepared films. All these methods gave consistent results for n to within an error of ±0.5%. The average values were used in the thickness determination.

As is well-known,[8] polystyrene shows a weak absorption around 4.8 eV (~2600 Å), which is a remnant of the forbidden absorption in benzene at about the same energy. Since this absorption was too weak to be observed even in the thickest of the films used in the observations described so far, an additional transmission measurement was performed in the vicinity of this band on a 4.50-μm thick film, and the extinction coefficient k for this band determined. The measurements were extended on this thick film down to 0.6 eV, where no further absorption was observed. This thick film was also used to determine the density of the polystyrene films. A known area of the film was cut out and weighed. The density was found to be 1.05 ± 0.02 g/cm^3. This value agrees with the literature values[8] for bulk polystyrene: 1.042–1.065 g/cm^3. The tacticity of polystyrene in our films was not checked. It does not, however, seem to affect the results in the present spectral region.[9] Errors in the results obtained for $(n-1)$ and k were estimated to be less than ±2%, except for the region above 60 eV.

The measurements described above were made with a Cary recording spectrophotometer (model 14) in the region 0.6–2 eV, a Seya-Namioka monochromator (McPherson model 235) in the region 2–15 eV, and a grazing-incidence monochromator (McPherson model 247) in the region 13–82 eV. Above 7.5 eV the measurements were made with line sources (hydrogen discharge and a condensed air spark) while below 7.5 eV continuum sources were employed.

III. RESULTS AND DISCUSSION

A. Extinction coefficient k

The results for k between 0.6 and 82 eV are presented in Fig. 1 on a logarithmic plot. The spectrum exhibits structure below 10 eV due to molecular electronic excitations. Above 10 eV, the spectrum is essentially structureless, except for a broad absorption peak at around 14 eV. The absorption decreases rapidly and monotonically above this peak, and can be described by a straight line above 20 eV on a logarithmic plot. The best fit of the present k values between 20 and 60 eV to a straight line gave the expression.

$$k(E)=7.81\times10^3E^{-3.23}, \tag{2}$$

where E is the photon energy in eV. Deviation

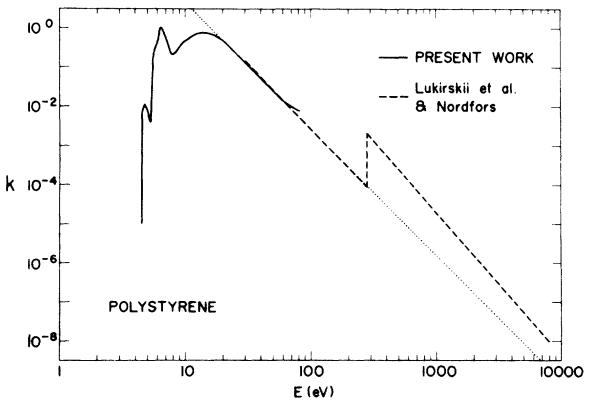

FIG. 1. Extinction coefficient k for polystyrene as a function of photon energy E. Dotted line is extrapolation of the present results between 20 and 60 eV.

found above 60 eV of the k values from the straight-line fit seems to be due to experimental errors in the transmission measurements in that region, where the transmittances of thin films were quite high.

Also shown in Fig. 1 are the combined results for k obtained by Lukirskii *et al.*[2] and by Nordfors[3] extending to the hard-x-ray region. These results were originally given by the expressions[2]

$$\mu(\lambda) = 0.40\lambda^{2.31} \tag{3}$$

for $44 < \lambda < 410$ Å and

$$\mu(\lambda) = 2.40\lambda^{2.68} \tag{4}$$

for $8 < \lambda < 44$Å, where μ is the linear absorption coefficient in cm^{-1} and λ is the wavelength of the photons in Å. In plotting these expressions in Fig. 1, they were converted into the forms

$$k(E) = 1.13 \times 10^{4} E^{-3.31} \tag{5}$$

for $30 < E < 282$ eV.

$$k(E) = 2.21 \times 10^{6} E^{-3.68} \tag{6}$$

for $282 < E < 1550$ eV, using the definition $\mu = 10^{8}(4\pi k/\lambda)$. Expressions (3) and (4) were deduced by Lukirskii *et al.*[2] from their experimental absorption measurements. The results of Nordfors[3] obtained in the region from 1490 to 8050 eV were found[10] to fit well to expressions (4) or (6) for the higher-energy region. Since, as will be shown, in the spectral region of their studies the refractive indices are quite close to unity, transmission measurements gave the absorption coefficient directly without taking into account reflection at the film boundaries. Their measurements were, however, made at only eight wavelengths from 30 to 282 eV, nine wavelengths from 282 to 1550 eV, and five wavelengths[10] from 1490 to 8050 eV, employing the characteristic x-rays from various anode materials.

The jump in absorption at 282 eV is due to the carbon K-shell absorption edge, in the vicinity of which some fine structure should be found. The study of fine structure in core shell absorption edges using a continuum source of synchrotron radiation is of current interest, but such studies are not available for polystyrene. Despite the coarseness of Lukirskii *et al.*'s and Nordfors's data, their results seem to represent the essential features and correct order of magnitude of the absorption for polystyrene over a very wide range of photon energies. Indeed a fairly close fit is found between the present results and Lukirskii *et al.*'s results in the low-energy region. The difference in k between the present result and their result is about 9% at 30 eV, and that between the extrapolation of the present result from 20 to 60 eV, which is shown by a dotted line in Fig. 1, and their result is about 8% at 282 eV. Two lines representing the extrapolations of the present results and their results below 282 eV cross at around 100 eV, indicating that the differences are not due to any systematic errors resulting from, for example, error in determination of the film thickness in either study, but due to random errors. Their original data at eight wavelengths below 282 eV, in fact, exhibit noticeable scatter from a straight-line fit even on a logarithmic plot, but the discrepancy of their expression (5) from our expression (2) is well within the 10% experimental uncertainty claimed by them for their original data.

The results for k given in Fig. 1 provide basic data for comprehensive information about the electronic response of polystyrene to electromagnetic radiation. Before deriving the other optical quantities from these results, the validity of the k values obtained here was checked by evaluating the sum rule[11]

$$N_1(E) = \frac{4}{\pi} \frac{m}{4\pi n_0 e^2 \hbar^2} \int_0^E E' k(E')\, dE' \rightarrow N, \quad E \rightarrow \infty, \tag{7}$$

where n_0 is the molecular density and N is the total number of electrons in a molecule. Taking a monomeric unit $-(C_8H_8)-$ of polystyrene as a molecular unit, N is 56. In carrying out integration (7), the k values above 8050 eV were assumed to be represented by expression (6) up to an infinite photon energy. This can be expected at least up to the MeV region, where photon attenuations due to the Compton effect and pair creation become appreciable.[12] In the region below 0.6 eV, where photoabsorption due to molecular vibrations occurs, the k values were assumed to be so small that the contribution of $E'k(E')$, in this low-energy region, to $N_1(E)$ could be neglected.

The results of calculations of $N_1(E)$ are plotted in Fig. 2 as a function of E. Since in this study it was difficult to determine experimentally the density of the polystyrene film ρ with an uncertainty less that ±2%, the molecular density $n_0 (= L\rho/M)$ was adjusted so that the value of $N_1(E)$ became equal to N in the limit of $E \rightarrow \infty$. (L is Avogadro's number and M is the molecular weight.) This gave a film density of 1.040 g/cm^3, which is in excellent agreement with the measured value of 1.05 ± 0.02 g/cm^3. Thus, in this check, the overall validity of the k values was confirmed with an uncertainty of ±1%.

Further evaluations of $N_1(E)$ were made on the k values due to the valence and core excitations, separately. A saw-tooth-like shape of the k spectrum in the logarithmic plot at high energy allows us to separate the absorption due to the core

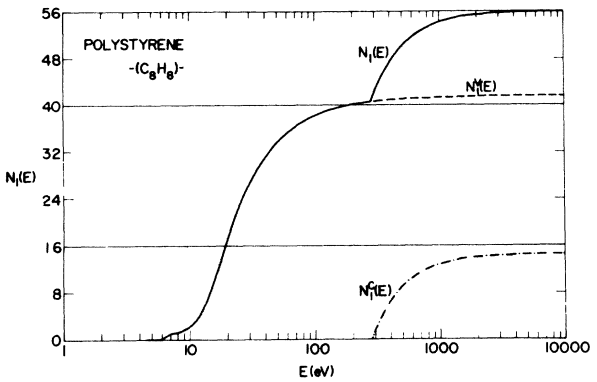

FIG. 2. Effective number of electrons $N_1(E)$ per monomeric unit of polystyrene obtained from the extinction coefficient k as a function of photon energy E. $N_1^v(E)$ and $N_1^c(E)$ represent the contributions from the valence and core electron excitations, respectively.

excitations from the total absorption. The separation was made simply by extrapolating the slope in Fig. 1 below the K-shell edge to higher energies. This seems to be a quite plausible procedure. The results of $N_1^v(E)$ and $N_1^c(E)$, the contributions to $N_1(E)$ from the valence and core excitations, respectively, are given in Fig. 2. It is noted that a redistribution of electron numbers corresponding to 1.51 electrons is found between the valence and core excitations. $N_1^v(E)$ and $N_1^c(E)$ should tend to 40 and 16, the numbers of valence and core electrons, respectively, in the limit $E \to \infty$, if there is no oscillator strength coupling between them. The fact that the oscillator strengths for inner shells are considerably smaller than their numbers of electrons has been known since the early days of x-ray spectroscopy.[13] In addition the magnitude of the oscillator strength redistribution between the outer and inner shells has been known, in general, to become larger as the atomic number becomes bigger. It is further to be noted that the effective numbers of electrons as plotted in Fig. 2 as functions of photon energy E do not saturate until a few thousand eV. This is so even for the valence electrons showing that even at these high energies the contribution of valence excitations to the oscillator strength is not negligible.

The analyses presented above were performed on the present results between 0.6 and 60 eV. In the region from 60 to 282 eV, the extrapolation of the present results between 20 and 60 eV expressed by Eq. (2) was used, instead of Lukirskii *et al.*'s result given by Eq. (5) for the reason mentioned earlier. Expression (2) was also used to represent the absorption by valence electrons above 282 eV. If we used Lukirskii *et al.*'s expression (5) for the absorption by valence electrons above 60 eV, no substantial change is found in the results for the film density and the oscillator strength redistribution. In all further analyses presented below, therefore our expression (2) was used for the absorption by valence electrons above 60 eV. Some uncertainties in the sum rule calculations may arise from the ambiguity of the k data in the vicinity of the carbon K-absorption edge at around 282 eV. In the present analyses, a steplike edge was assumed at 282 eV as given by Lukirskii *et al.* Since such a sharp K edge has been observed for polypropylene[14] $[-(C_3H_6)-]$, an organic polymer similar to polystyrene, at 283 eV using a continuum of soft x-ray photons from a synchrotron, the threshold energy used in the present analyses seems to be reasonable. A ±2-eV deviation of the threshold energy from 282 eV results in changes of only ±0.003 g/cm^3 and ∓0.13 electrons in the results for the film density and the oscillator strength redistribution, respectively. Thus, although to evaluate the uncertainty involved in the present results we have to wait for a precise observation of the carbon K-edge structure in polystyrene the present results seen to be sufficiently correct with uncertainties which are probably less than those suggested.

B. Refractive index n

The refractive index $n(E)$ at a photon energy E can be determined by the Kramers-Kronig relation

$$n(E)-1=\frac{2}{\pi}\int_0^\infty \frac{E'k(E')}{E'^2-E^2}\,dE', \tag{8}$$

using the experimental values of k at all energies. In the present case, the experimental k values in the region from 0.6 to 8050 eV are available, and in the regions outside these energies the values extrapolated as described earlier in the sum rule calculation can be used. $n(E)$, therefore, can be determined with little uncertainty at all energies. Just as k can be separated into the valence and core contributions, $n(E)-1$ is also separable. The results of $n^v(E)-1$ and $n^c(E)-1$, the contributions to $n(E)-1$ from the valence and core excitations, respectively, are presented in Figs. 3 and 4, respectively.

Both $n^v(E)-1$ and $n^c(E)-1$ become almost constant in the regions far below the absorption onsets. It is to be noted that the values of $n^c(E)-1$ below about 100 eV are smaller than those of $|n^v(E)-1|$ in that region by a factor 10^3 or so, showing that the contribution of the core excitation to the refractive index is negligibly small in

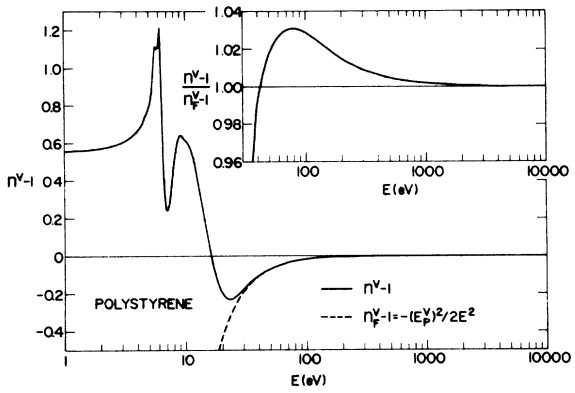

FIG. 3. Refractive index for polystyrene due to the valence electron excitations as a function of photon energy E. Dashed curve represents the free-electron values.

this low energy region. The singularity appearing in $n^c(E)-1$ at the carbon K edge is due to the present approximation of a steplike onset for the K-shell absorption. At high energies, $n^v(E)-1$ and $n^c(E)-1$ tend to zero.

As will be shown later in the Appendix, if the $k(E)$ values are expressed for $E \geq E_1$ by a form

$$k(E) = \alpha E^{-\beta}, \tag{9}$$

as has indeed been found in the present results for $E_1 \simeq 20$ eV, $n(E)-1$ for $E \geq 10E_1$ can be written

$$n(E)-1 = -E_p^2/2E^2 - Q(\beta)k(E), \tag{10}$$

with an accuracy much better than 99%, where E_p^2 is a constant defined by sum rule (7) as

$$E_p^2 = \frac{4}{\pi}\int_0^\infty E'k(E')\,dE' = \frac{4\pi n_0 e^2\hbar^2}{m} N_1, \tag{11}$$

and $Q(\beta)$ is a quantity which depends only on the exponent β in expression (9). The plot of $Q(\beta)$ vs β given in the Appendix (Fig. 12) shows that for $\beta > 2$ as in the present results, $n(E)-1$ goes asymptotically to

$$n(E)-1 = -E_p^2/2E^2 \tag{12}$$

at high energies. This form of $n(E)-1$ is that of a free-electron gas in the high-energy limit. In the present case, using the expressions $k^v(E) = 7.81\times10^3 E^{-3.23}$ and $k^c(E) = 2.21\times10^6 E^{-3.68} - 7.81\times10^3 E^{-3.23}$, $n^v(E)-1$ and $n^c(E)-1$ were obtained for $E \geq 200$ eV and $E \geq 2820$ eV, respectively, as

$$n^v(E)-1 = -(E_p^v)^2/2E^2 - 1.78\times10^3/E^{3.23}, \tag{13}$$

$$n^c(E)-1 = -(E_p^c)^2/2E^2 - 1.85\times10^6/E^{3.68} + 1.78\times10^3/E^{3.23}, \tag{14}$$

where $(E_p^v)^2 = (4\pi n_0 e^2\hbar^2/m)\times41.51$ and $(E_p^c)^2 = (4\pi n_0 e^2\hbar^2/m)\times14.49$. The detailed behavior of $n^v(E)-1$ and $n^c(E)-1$ at high energies relative to the free-electron expressions $n_F^v(E)-1 = -(E_p^v)^2/2E^2$ and $n_F^c(E)-1 = -(E_p^c)^2/2E^2$, respectively, are shown in the insets of Figs. 3 and 4.

The results of $[n^v(E)-1]/[n_F^v(E)-1]$ and $[n^c(E)-1]/[n_F^c(E)-1]$ given here exhibit quite similar behaviors and show that monotonic convergences of $n^v(E)-1$ and $n^c(E)-1$ to the respective free-electron values start at about 100 and 900 eV, respectively. It is to be noted, however, that the deviation of $n^c(E)-1$ values from the free-electron values is considerably larger than that of $n^v(E)-1$ over the entire high energy region. The relatively close fit of the $n^v(E)-1$ values to the free-electron values above 40 eV in Fig. 3 has to be considered fortuitous. As is shown in the Appendix (Fig. 12), this close fit is due to the relatively small value of $Q(\beta)$ in Eq. (10) for $\beta = 3.23$, the exponent for absorption of the valence electrons.

A simple and interesting sum rule

$$S(E) = \int_0^E [n(E')-1]\,dE' \to 0, \quad E \to \infty \tag{15}$$

has been derived recently by Altarelli *et al.*[5] for the refractive index $n(E)$ of isotropic media including conductors. This sum rule asserts that the average value of the refractive index over the whole spectral range is equal to unity. In the derivation of this sum rule, the only assumption made was that in the high-energy limit the medium responds like a free-electron gas, i.e.,

$$n(E) + ik(E) \simeq 1 - E_p^2/2E^2. \tag{16}$$

As we have already seen, this is indeed the case for the present results. $S(E)$ evaluated from $n^v(E)-1$ and $n^c(E)-1$ are given in Fig. 5 as functions of photon energy E up to 10^4 eV. Both $S^v(E)$ and $S^c(E)$ converge slowly to zero at high ener-

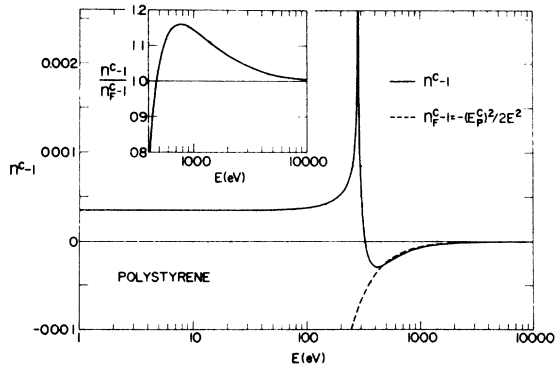

FIG. 4. Refractive index for polystyrene due to the carbon core electron excitations as a function of photon energy E. Dashed curve represents the free-electron values.

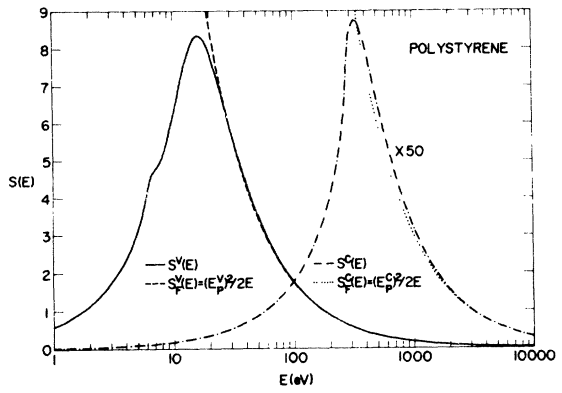

FIG. 5. Sum rule $S(E)$ for the refractive index n of polystyrene as a function of photon energy E. $S^v(E)$ and $S^c(E)$ represent the contributions from the valence and core electron excitations, respectively. $S_F^v(E)$ and $S_F^c(E)$ represent the corresponding free-electron values.

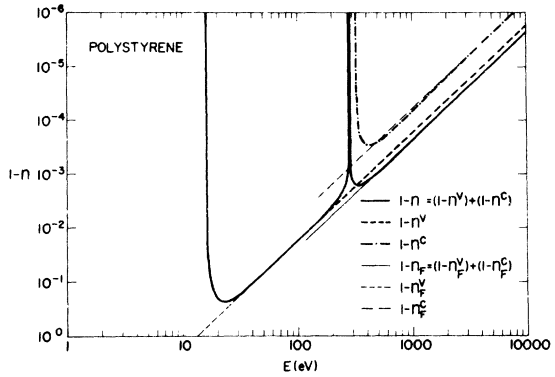

FIG. 6. Refractive index n for polystyrene in the region where $n-1$ is negative as a function of photon energy E. n^v and n^c represent the contributions from the valence and core electron excitations, respectively. n_F, n_F^v, and n_F^c represent the corresponding free-electron values.

gies. The analytical expressions (13) and (14) allow us to extend the integrations $S^v(E)$ and $S^c(E)$ up to infinity. It was found that both $S^v(E)$ and $S^c(E)$ converge exactly to zero in the limit of $E \to \infty$.

For a high energy E, above which the behavior of $n(E)-1$ can be represented by the free-electron expression (12), $S(E)$ may be approximated by

$$S_F(E) = -\int_E^\infty [n(E')-1]\,dE' \simeq \frac{E_p^2}{2E}. \tag{17}$$

This form describes the asymptotic behavior of $S(E)$ in the high-energy limit. $S_F(E)$ from the valence and core contributions are presented in Fig. 5 and compared with the results for $S(E)$. $S(E)$ is described well by $S_F(E)$ over a wide range in the high-energy region. Relative deviations between $S(E)$ and $S_F(E)$ are, however, about the same as those found in the results for $[n(E)-1]/[n_F(E)-1]$ at corresponding energies as shown in the inserts of Figs. 3 and 4.

Before closing this subsection, we present in Fig. 6 the results of $n(E)-1$, in the region where $n(E)-1$ is negative, on logarithmic plots, together with the free-electron values. These plots are of help in evaluating the complex dielectric function and the energy loss function, which will be presented in Sec. III C.

C. Complex dielectric function ϵ and the energy-loss function $\mathrm{Im}(-1/\epsilon)$

The imaginary part of the complex dielectric function $\epsilon(=\epsilon_1+i\epsilon_2)$ and the energy-loss function $\mathrm{Im}(-1/\epsilon)$ for fast charged particles were calculated from the values of n and k, and are presented in Fig. 7 on logarithmic plots, together with the values of $2k$. Among these three spectra, substantial differences are found only in the low-energy region. Deviations of the $\mathrm{Im}(-1/\epsilon)$ spectrum from ϵ_2, found in the low energy region, describe the so-called collective effect,[15] i.e., charged particle density fluctuations brought about by fast charged particles incident on condensed matter. In Fig. 7, regularities in the displacement of the low-energy structures should be noted. All three peaks found in the low-energy region shift to higher energies in order of ϵ_2, $2k$, and $\mathrm{Im}(-1/\epsilon)$, and their peak heights decrease also in this order.

For ϵ_2 and $\mathrm{Im}(-1/\epsilon)$, there exist the well-known f sum rules[4]

$$N_2(E) = \frac{2}{\pi}\frac{m}{4\pi n_0 e^2\hbar^2}\int_0^E E'\epsilon_2(E')\,dE' \to N, \quad E \to \infty, \tag{18}$$

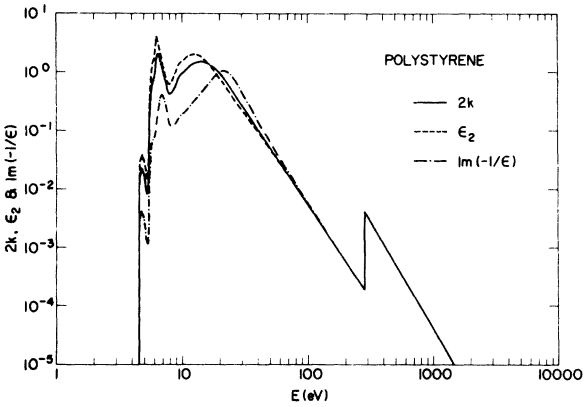

FIG. 7. Twice the extinction coefficient k, the imaginary part of the complex dielectric function $\epsilon(=\epsilon_1+i\epsilon_2)$ and the energy-loss function $\mathrm{Im}(-1/\epsilon)$ for polystyrene as functions of photon energy E.

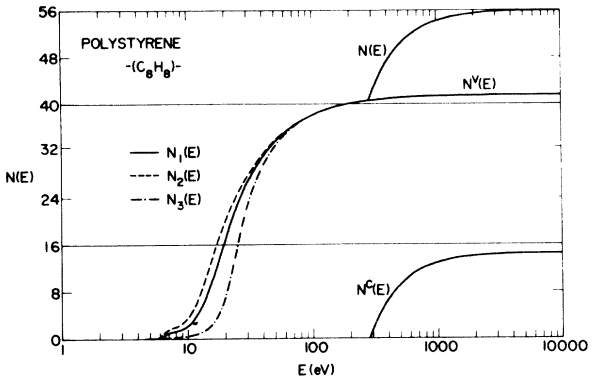

FIG. 8. Effective number of electrons $N_1(E)$, $N_2(E)$, and $N_3(E)$ per monomeric unit of polysytrene obtained from the extinction coefficient k, the imaginary part of the complex dielectric function $\epsilon\,(=\epsilon_1+i\epsilon_2)$ and the energy-loss function $\mathrm{Im}(-1/\epsilon)$, respectively, as functions of photon energy E. $N^v(E)$ and $N^c(E)$ represent the contributions from the valence and core electron excitations, respectively.

$$N_3(E)=\frac{2}{\pi}\frac{m}{4\pi n_0 e^2\hbar^2}\int_0^E E'\,\mathrm{Im}\left(\frac{-1}{\epsilon(E')}\right)dE'\to N,\quad E\to\infty, \tag{19}$$

The results of $N_2(E)$ and $N_3(E)$ are shown in Fig. 8 as functions of photon energy E, together with that of $N_1(E)$ which has already been presented in Fig. 2. It was found that all these numbers of effective electrons converge to the same value in the high-energy limit. As has been seen, k and $n-1$ are separable into the valence and core contributions. Generally, ϵ_2 and $\mathrm{Im}(-1/\epsilon)$ are not separable, as by definition they include the cross terms between the valence and core contributions. In the case of $|n^v-1|$ and $|n^c-1|\ll 1$, and k^v and $k^c\ll 1$,

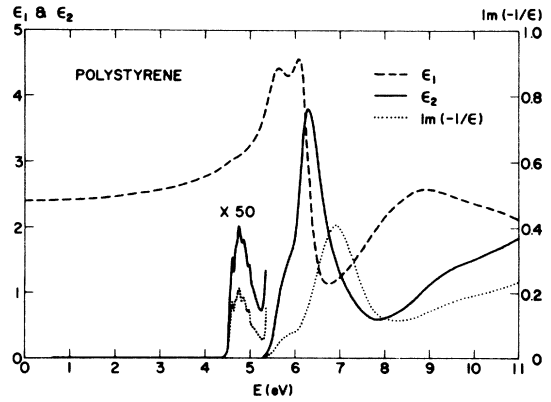

FIG. 9. Real and imaginary parts of the complex dielectric function $\epsilon\,(=\epsilon_1+i\epsilon_2)$ and the energy-loss function $\mathrm{Im}(-1/\epsilon)$ for polysytrene as functions of photon energy E.

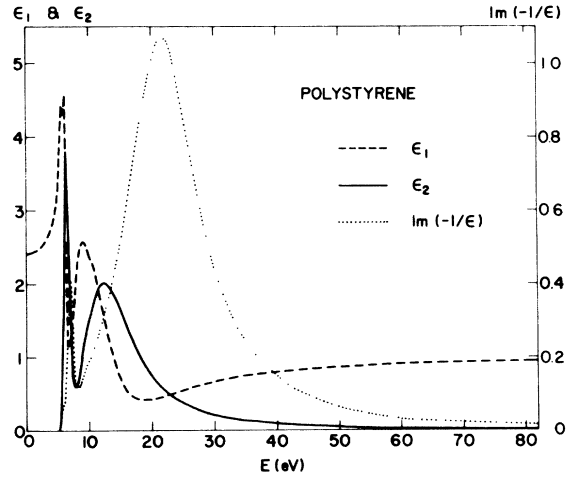

FIG. 10. Real and imaginary parts of the complex dielectric function $\epsilon\,(=\epsilon_1+i\epsilon_2)$ and the energy-loss function $\mathrm{Im}(-1/\epsilon)$ for polysytrene as functions of photon energy E.

however, it can be shown that ϵ_2 and $\mathrm{Im}(-1/\epsilon)$ are separable. This can be seen from the results shown in Fig. 7, where ϵ_2 and $\mathrm{Im}(-1/\epsilon)$ are in agreement with $2k$ in the high-energy region; thus they can be separated into the valence and core contributions in the same manner as the k spectrum. $N_1(E)$, $N_2(E)$, and $N_3(E)$ for the valence and core contributions are plotted in Fig. 8. Because of the close agreement among $2k$, ϵ_2, and $\mathrm{Im}(-1/\epsilon)$, no substantial differences were found in the $N(E)$ values in the high-energy region.

Detailed spectra for ϵ_1, ϵ_2, and $\mathrm{Im}(-1/\epsilon)$ in the low-energy region are presented in Figs. 9 and 10 on linear plots. The general spectral features given here agree well with results from earlier studies[9,16-20] obtained below 20 eV. Considerable numerical disagreements are, however, found between the present results and some of the earlier ones. Apparently, the discrepancies can be attributed to poor experimental accuracy and large uncertainties in data analysis in the earlier studies. Four absorption bands can be distinguished below 11 eV in the ϵ_2 spectrum shown in Fig. 9; at around 4.8, 5.8, 6.3, and 9.5 eV. The interpretation of these structures and the corresponding structures in $\mathrm{Im}(-1/\epsilon)$ have already been described by many authors.[9,16-20] The spectral features in the extreme ultraviolet above 10 eV given in Fig. 10 are quite simple and are marked only by the broad peaks at 12.5 eV in ϵ_2 and at 21.7 eV in $\mathrm{Im}(-1/\epsilon)$. These features are typical of many organic solids.[6,7,21,22] The spectrum for $\mathrm{Im}(-1/\epsilon)$ shown here agrees well with that from characteristic electron energy-loss measurements[16,23] on thin polystyrene films.

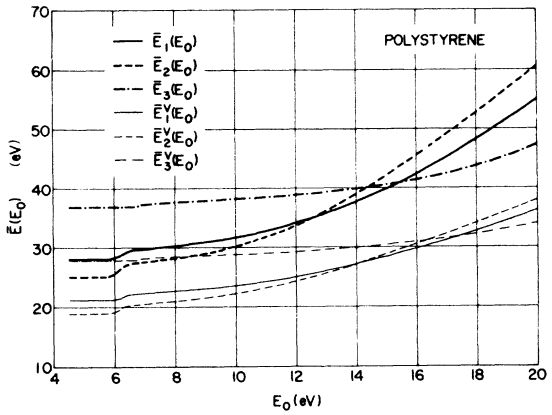

FIG. 11. Average photoexcitation energy $\bar{E}_2$ and the average energy loss $\bar{E}_3$ for polystyrene over the spectral range from E_0 to infinity as functions of E_0. $\bar{E}_1$ may represent $\bar{E}_2$ and $\bar{E}_3$ in the low-density limit. $\bar{E}_1^v$, $\bar{E}_2^v$, and $\bar{E}_3^v$ represent the corresponding values due to the valence electron excitations only.

D. Average photoexcitation energy and the average energy loss

The present results, extending substantially over the region from zero to infinite photon energy, allow us to evaluate the average photoexcitation energy and the average energy loss suffered by fast charged particles. These quantities are of key importance in radiation physics which deals with the interaction of high-energy ionizing radiations with matter.

Shown in Fig. 11 are the results of the photoexcitation energy $\bar{E}_2(E_0)$ and the energy loss $\bar{E}_3(E_0)$ averaged over the spectral region from E_0 to infinity, i.e.,

$$\bar{E}_2(E_0)=\int_{E_0}^{\infty} E\epsilon_2(E)\,dE \Big/ \int_{E_0}^{\infty} \epsilon_2(E)\,dE\,, \tag{20}$$

$$\bar{E}_3(E_0)=\int_{E_0}^{\infty} E\,\mathrm{Im}\left(\frac{-1}{\epsilon(E)}\right)dE \Big/ \int_{E_0}^{\infty} \mathrm{Im}\left(\frac{-1}{\epsilon(E)}\right)dE\,. \tag{21}$$

Such plots of $\bar{E}_2(E_0)$ and $\bar{E}_3(E_0)$ as functions of E_0 are of help in evaluating the contribution of excitations in a particular energy range to the average excitation energy and energy loss. Since, in the present results, the onset of valence absorption was found at 4.5 eV, the values of $\bar{E}_2(E_0)$ and $\bar{E}_3(E_0)$ at $E_0=4.5$ eV give the average excitation energy and energy loss, respectively, over the entire oscillator strength distribution. $\bar{E}_2$ and $\bar{E}_3$ at $E_0=4.5$ eV were found to be 25.1 and 36.8 eV, respectively. This difference can be attributed to an energy loss associated with the creation of collective oscillations due to the interaction of fast charged particles with matter. Photons generally do not excite collective oscillations in experimental systems designed for the measurement of k.

From the definition of the energy-loss function,[15] the average energy loss $\bar{E}_3(E_0)$ obtained here should be considered to be that due to a single energy-loss event associated with zero transverse momentum transfer from the fast charged particle to the medium. Therefore, it cannot be compared directly with similar quantities such as the mean excitation potential I appearing in the well-known Bethe-Bloch formula[24,25] for the stopping power or the so-called W value, the average energy for an ion-pair creation. It may be worthwhile, however, to note that $I=63.5$ eV was obtained by Sternheimer[26] for polystyrene, and $W=37$ eV was reported by Mathieu *et al.*[27] for liquid cyclohexane, which may be considered to be a model system for solid polystyrene.

The variations of $\bar{E}_2(E_0)$ and $\bar{E}_3(E_0)$ shown in Fig. 11 as functions of E_0 are no more than a few eV for $E_0 \leq 10$ eV, showing that the contributions of such low-energy excitations to the average excitation energy and energy loss are relatively small. This result will apply to other condensed hydrocarbons, as substantial differences of the oscillator strength distribution for these materials have been found[21] only in the region below about 10 eV. Also shown in Fig. 11 is $\bar{E}_1(E_0)$ defined by

$$\bar{E}_1(E_0)=\int_{E_0}^{\infty} Ek(E)\,dE \Big/ \int_{E_0}^{\infty} k(E)\,dE\,. \tag{22}$$

As is well known, $Ek(E)$ for condensed media cannot be considered to give the oscillator strength distribution in a strict sense. It has been found for many hydrocarbons,[9,28,29] however, that, except for molecular Rydberg fine structure, the k spectrum in the gas phase agrees well with that in the condensed phase apart from a constant factor corresponding to the ratio of molecular densities between these two phases. This is particularly so in the region above 10 eV, where most of the excitation energy and energy loss occurs. $\bar{E}_1(E_0)$ shown here, therefore, can be regarded as representing approximate values of $\bar{E}_2(E_0)$ and $\bar{E}_3(E_0)$ in the low-density limit, i.e., for gas-phase hydrocarbons, since ϵ_2 and $\mathrm{Im}(-1/\epsilon)$ in the low-density limit agree with $2k$ over the whole spectral range. $\bar{E}_1^v(E_0)$, $\bar{E}_2^v(E_0)$, and $\bar{E}_3^v(E_0)$ presented in Fig. 11 are the respective averages derived from the valence excitation only. Here, one may see how much the core excitations contribute to the average excitation energy and energy loss.

Finally the values of the extinction coefficient k obtained and used in this study are tabulated in Table I for further use.

TABLE I. Extinction coefficient k for polystyrene as a function of photon energy E.

E (eV)	k	E (eV)	k
0.6		11.0	0.586
⋮	0.000 00	11.5	0.636
4.4		12.0	0.681
4.5	0.0011	12.5	0.713
4.6	0.0089	13.0	0.730
4.7	0.0103	13.5	0.743
4.8	0.0103	14.0	0.748
4.9	0.0092	14.5	0.747
5.0	0.0072	15.0	0.741
5.1	0.0054	16.0	0.702
5.2	0.0041	17.0	0.646
5.3	0.0043	18.0	0.590
5.4	0.0292	19.0	0.531
5.6	0.183	20.0	0.473
5.8	0.330	22.0	0.361
6.0	0.431	24.0	0.276
6.2	0.825	26.0	0.211
6.4	1.023	28.0	0.164
6.6	0.884	30.0	0.129
6.8	0.694	35.0	0.0806
7.0	0.524	40.0	0.0542
7.3	0.354	45.0	0.0375
7.6	0.239	50.0	0.0247
7.9	0.206	55.0	0.0192
8.2	0.220	60.0	0.0136
8.6	0.264	⋮	a
9.0	0.344	282	
9.5	0.425	⋮	b
10.0	0.474	8050	
10.5	0.523		

[a] $k = 7.81 \times 10^3 E^{-3.23}$ (extrapolation of k between 20 and 60 eV).

[b] $k = 2.21 \times 10^6 E^{-3.68}$ (Refs. 2 and 3).

E. Concluding remarks

It was found in the present study that the convergence of all sum rules associated with the optical constants of polystyrene are quite slow, and the almost perfect saturations do not occur until the keV region. This is for a material having one of the simplest of all electronic configurations. Experimentally, the f sum rules have provided useful criteria for consistency checks of the optical constants. It has been shown, however, that the f sum rules are applicable only when the experimental data cover all electronic excitations including the innermost core excitations. In applying the f sum rules for a particular shell, difficulties arise from, in addition to the slow convergences, the fact that a non-negligible amount of oscillator strength coupling always occurs between the inner- and outer-shell electrons. If experimental data cover only a part of the total oscillator strength distribution as is so in most cases, the oscillator strength for a particular shell, to which the f sum rules should converge, cannot be known a priori without knowing those for the remaining shells. It has been proposed recently by Altarelli *et al.*[5] that the $S(E)$ sum rule for the refractive index given by Eq. (15) may be used as a saturation criterion and/or as a consistency check for the optical constants obtained experimentally. The present results for $S(E)$ shown in Fig. 5, indeed, converge to the free-electron values $S_F(E)$ given by Eq. (17) much faster than the f sum rules converge. Differences between $S(E)$ and $S_F(E)$, however, are not negligibly small up to quite high energies. Further, E_p^2 for a particular shell in the expression for $S_F(E)$, which is proportional to the oscillator strength, cannot be known until the convergence of the f sum rule is attained. Practically, the new sum rule for $S(E)$, if applied to a particular shell, is subject to the same uncertainty as the f sum rules.

APPENDIX

Let us assume that the extinction coefficient $k(E)$ at photon energy E is expressed by

$$k(E) = \alpha E^{-\beta} \tag{A1}$$

for $E \geq E_1$ as is generally found for high photon energies, where α and β are positive constants. According to a Kramers-Kronig relation, the refractive index $n(E)$ at photon energy E is given by

$$n(E) - 1 = \frac{2}{\pi} \int_0^\infty \frac{E' k(E')}{E'^2 - E^2}\, dE' . \tag{A2}$$

Dividing the integration into three regions, and, then, allowing less than 1% error to the first and third regions, $n(E)-1$ can be written

$$n(E) - 1 = \frac{2}{\pi}\left(\int_0^{0.1E} \frac{E' k(E')}{E'^2 - E^2}\, dE' + \int_{0.1E}^{10E} \frac{E' k(E')}{E'^2 - E^2}\, dE' + \int_{10E}^{\infty} \frac{E' k(E')}{E'^2 - E^2}\, dE' \right)$$

$$= \frac{2}{\pi}\left(-\frac{1}{E^2} \int_0^{0.1E} E' k(E')\, dE' + \int_{0.1E}^{10E} \frac{E' k(E')}{E'^2 - E^2}\, dE' + \int_{10E}^{\infty} \frac{k(E')}{E'}\, dE' \right). \tag{A3}$$

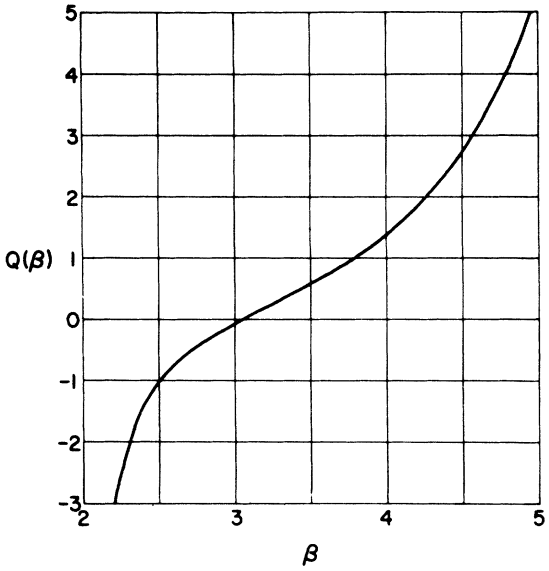

FIG. 12. Dependence of $Q(\beta)$ on the exponent β.

Now, if we confine ourselves to the case of $E \geq 10E_1$. The first integral can be written

$$\frac{2}{\pi}\frac{1}{E^2}\left(-\int_0^{\infty} E'k(E')\,dE' + \int_{0.1E}^{\infty} E'k(E')\,dE'\right). \tag{A4}$$

The first integral in (A4) should be a constant from the sum rule, and the second one is calculable analytically, as the expression (A1) holds for this region. Thus, the integrals in (A4) become

$$\frac{-E_p^2}{2E^2} + \frac{2}{\pi}\frac{10^{\beta-2}}{\beta-2}k(E), \tag{A5}$$

where E_p^2 is defined by

$$E_p^2 = \frac{4}{\pi}\int_0^{\infty} E'k(E')\,dE'. \tag{A6}$$

The third integral in Eq. (A3) is also calculable analytically and is given by

$$(2/\pi)(10^{-\beta}/\beta)k(E). \tag{A7}$$

Finally, the second integral in Eq. (A3) is also calculable as the expression (A1) holds for this region. However, the functional dependence of this integral on E can be obtained easily without carrying out the integration. Using the similarity of the expression (A1) in logarithmic scale, the integral region from $0.1E$ to $10E$ can be shifted to an arbitrary region, for example, from $0.1E_2$ to $10E_2$. This shift introduces a factor $(E/E_2)^{-\beta}$, i.e.,

$$\frac{2}{\pi}\int_{0.1E}^{10E}\frac{E'k(E')}{E'^2-E^2}dE' = \frac{2}{\pi}\left(\frac{E}{E_2}\right)^{-\beta}\int_{0.1E_2}^{10E_2}\frac{E'k(E')}{E'^2-E_2^2}dE'. \tag{A8}$$

Since this shift of integral region is valid for any E_2 ($\geq E$), the integral

$$\frac{2}{\pi}\left(\frac{1}{E_2}\right)^{-\beta}\int_{0.1E_2}^{10E_2}\frac{E'k(E')}{E'^2-E_2^2}dE' \tag{A9}$$

should be a constant. Thus, the second integral in Eq. (A3) can be written

$$(2/\pi)P(\beta)k(E), \tag{A10}$$

where $P(\beta)$ defined by

$$P(\beta) = \left(\frac{1}{E_2}\right)^{-\beta}\int_{0.1E_2}^{10E_2}\frac{E'^{-\beta+1}}{E'^2-E_2^2}dE' \tag{A11}$$

is a quantity depending only on β. Summing up (A5), (A7), and (A10), we have for $E \geq 10E_1$,

$$n(E) - 1 = -\frac{E_p^2}{2E^2} + \frac{2}{\pi}\left(\frac{10^{\beta-2}}{\beta-2} + P(\beta) + \frac{10^{-\beta}}{\beta}\right)k(E) = -\frac{E_p^2}{2E_2} - Q(\beta)k(E). \tag{A12}$$

Values of $Q(\beta)$ obtained from a numerical calculation of $P(\beta)$ are plotted in Fig. 12 as a function of β. $Q(\beta)$ becomes zero at $\beta = 3.06$ and goes to negative infinity in the limit of $\beta \to 2$. Such an analytical expression for $n(E) - 1$ for the high-energy region is quite useful in analyses of optical data as has been shown in this study, and can be applicable for any kind of material, as the expression (A1) involves a general behavior of k due to high-energy absorptions.

---

*Part of this work performed while on a Postdoctoral appointment in the Dept. of Physics, The University of Tennessee, Knoxville, Tenn.

†Operated by the Energy Research and Development Administration under Contract with the Union Carbide Corp.

[1]H. R. Philipp and H. Ehrenreich, J. Appl. Phys. 35, 1416 (1964); M. Altarelli and D. Y. Smith, Phys. Rev. B 9, 1290 (1974).

[2]A. P. Lukirskii, V. A. Fomichev, and I. A. Brytov, Opt. Spectry. (USSR) 20, 202 (1966).

[3]B. Nordfors, Ark. Fys. 11, 587 (1957).

[4]P. Nozières and D. Pines, Phys. Rev. 113, 1254 (1959).

[5]M. Altarelli, D. L. Dexter, H. M. Nussenzveig, and D. Y. Smith, Phys. Rev. B 6, 4502 (1972).

[6]T. Inagaki, R. N. Hamm, E. T. Arakawa, and L. R.

Painter, J. Chem. Phys. 61, 4246 (1974).
[7]T. Inagaki, R. N. Hamm, E. T. Arakawa, and R. D. Birkhoff, Biopolymers 14, 839 (1975).
[8]R. H. Boundy and R. F. Boyer, *Styrene, Its Polymers, Copolymers, and Derivatives* (Reinhold, New York, 1952).
[9]R. H. Partridge, J. Chem. Phys. 47, 4223 (1967).
[10]Apparently, the results cited in the figure in Lukirskii *et al.*'s paper (Ref. 2) as the results by Nordfors (Ref. 3) are not the Nordfors results, but those of empirical calculations by J. A. Victoreen [J. Appl. Phys. 20, 1141 (1949)]. Despite this erroneous citation, the original data taken by Nordfors at five wavelengths from 8.23 to 1.54 Å were found to fit well to the expression (4) or (6).
[11]F. Stern, *Solid State Physics*, edited by F. Sietz and D. Turnbull (Academic, New York, 1963), Vol. 15, p. 341.
[12]W. Heitler, *The Quantum Theory of Radiation* (Oxford U. P., Oxford, 1954), Chap. 7.
[13]A. H. Compton and S. K. Allison, X-Rays in Theory and Experiment (Van Nostrand, New York, 1936), p. 542.
[14]W. Hayes and F. C. Brown, Phys. Rev. A 6, 21 (1972).
[15]H. Raether, *Springer Tracts in Modern Physics*, edited by G. Höhler (Springer, Berlin, 1965), Vol. 38, p. 85.
[16]N. Swanson and C. J. Powell, J. Chem. Phys. 39, 630 (1963); Phys. Rev. 145, 195 (1966).
[17]J. G. Carter, T. M. Jelinek, R. N. Hamm, and R. D. Birkhoff, J. Chem. Phys. 44, 2266 (1966).
[18]J. T. Shapiro and R. P. Madden, J. Opt. Soc. Am. 58, 771 (1968).
[19]W. L. Buck, B. R. Thomas, and A. Weinreb, J. Chem. Phys. 48, 549 (1968).
[20]S. Onari, J. Phys. Soc. Jpn. 26, 500 (1969).
[21]T. Okabe, J. Phys. Soc. Jpn. 35, 1496 (1973).
[22]M. Isaacson, J. Chem. Phys. 56, 1803 (1972).
[23]R. E. Lavilla and H. Mendlowitz, J. Phys. (Paris) 25, 114 (1964).
[24]H. A. Bethe, *Handbuch der Physik* (Springer, Berlin, 1933), Vol. 24, p. 273.
[25]F. Block, Z. Phys. 81, 363 (1933).
[26]R. M. Sternheimer, Phys. Rev. 103, 511 (1956).
[27]J. Mathieu, D. Blanc, P. Caminade, and J. P. Patau, J. Chim. Phys. 64, 1679 (1967).
[28]E. E. Kock and M. Skibowski, Chem. Phys. Lett. 9, 429 (1971).
[29]M. Yoshino, J. Takeuchi, and H. Suzuki, J. Phys. Soc. Jpn. 34, 1039 (1973).